

# Virus-Induced Gene Silencing of Plastidial Soluble Inorganic Pyrophosphatase Impairs Essential Leaf Anabolic Pathways and Reduces Drought Stress Tolerance in *Nicotiana benthamiana*<sup>1[W][OA]</sup>

Gavin M. George, Margaretha J. van der Merwe, Adriano Nunes-Nesi, Rolene Bauer<sup>2</sup>, Alisdair R. Fernie, Jens Kossmann, and James R. Lloyd\*

Institute of Plant Biotechnology, University of Stellenbosch, Matieland 7602, Stellenbosch, South Africa (G.M.G., M.J.v.d.M., R.B., J.K., J.R.L.); and Max Planck Institute of Molecular Plant Physiology, D-14476 Potsdam-Golm, Germany (A.N.-N., A.R.F.)

The role of pyrophosphate in primary metabolism is poorly understood. Here, we report on the transient down-regulation of plastid-targeted soluble inorganic pyrophosphatase in *Nicotiana benthamiana* source leaves. Physiological and metabolic perturbations were particularly evident in chloroplastic central metabolism, which is reliant on fast and efficient pyrophosphate dissipation. Plants lacking plastidial soluble inorganic pyrophosphatase (psPPase) were characterized by increased pyrophosphate levels, decreased starch content, and alterations in chlorophyll and carotenoid biosynthesis, while constituents like amino acids (except for histidine, serine, and tryptophan) and soluble sugars and organic acids (except for malate and citrate) remained invariable from the control. Furthermore, translation of Rubisco was significantly affected, as observed for the amounts of the respective subunits as well as total soluble protein content. These changes were concurrent with the fact that plants with reduced psPPase were unable to assimilate carbon to the same extent as the controls. Furthermore, plants with lowered psPPase exposed to mild drought stress showed a moderate wilting phenotype and reduced vitality, which could be correlated to reduced abscisic acid levels limiting stomatal closure. Taken together, the results suggest that plastidial pyrophosphate dissipation through psPPase is indispensable for vital plant processes.

Pyrophosphate (PP<sub>i</sub>) is a key metabolite generated in the activation of several polymerization steps (Geigenberger et al., 1998; Stitt, 1998; Rojas-Beltrán et al., 1999; Farré et al., 2001; Sonnewald, 2001; López-Marqués et al., 2004), and its removal is essential to prevent the inhibition of thermodynamically unfavorable reactions (Geigenberger et al., 1998; López-Marqués et al., 2004). PP<sub>i</sub> is generally removed by inorganic pyrophosphatases, which hydrolyze PP<sub>i</sub> to orthophosphate (P<sub>i</sub>). Pyrophosphatases are ubiquitous in plant cells and found both as soluble forms in the

cytosol and plastid and as membrane-bound forms on the tonoplast (Rea and Poole, 1993; Baltscheffsky et al., 1999; Maeshima, 2000), mitochondria (Vianello and Macrì, 1999), and chloroplast (Jiang et al., 1997). In *Arabidopsis* (*Arabidopsis thaliana*), six soluble pyrophosphatase (sPPase) isoforms have been identified to date (Schulze et al., 2004). Five (*AtPPa1*, -2, -3, -4, and -5) are far more similar to each other than to *AtPPa6* (Schulze et al., 2004) and have been shown to be localized to the cytosol using GFP fusions (Ergen, 2006). In potato (*Solanum tuberosum*), two sPPase genes, *StPPa1* and *StPPa2*, which are similar to *AtPPa1*, have also been identified and demonstrated to be present in the cytosol using immunogold labeling (Rojas-Beltrán et al., 1999). In addition to sPPases, several other cytosolic enzymes can remove PP<sub>i</sub>, including the soluble enzymes pyrophosphate:Fru 6-P phosphotransferase and UDP-Glc pyrophosphorylase. Due to a lack of adverse phenotypic alterations found when altering the expression of these enzymes in autotrophic sink metabolism, a considerable degree of redundancy in cytosolic PP<sub>i</sub> catabolism has been proposed (Hajirezaei et al., 1994; Paul et al., 1995).

Heterologous studies aimed at elucidating the biological role of PP<sub>i</sub> in plants demonstrated to date that cytosolically expressed *Escherichia coli* sPPase leads to major effects on carbohydrate partitioning between Suc and starch (Sonnewald, 1992; Geigenberger et al.,

<sup>1</sup> This work was supported by grants from the South African National Research Foundation (to M.J.v.d.M., R.B., and J.R.L.) under the research theme Genetic Tailoring of Biopolymers (to G.M.G. and J.K.).

<sup>2</sup> Present address: Institute for Microbial Biotechnology and Metagenomics, Department of Biotechnology, University of the Western Cape, Private Bag X17, Bellville 7535, Cape Town, South Africa.

\* Corresponding author; e-mail lloyd@sun.ac.za.

The author responsible for distribution of materials integral to the findings presented in this article in accordance with the policy described in the Instructions for Authors (www.plantphysiol.org) is: James R. Lloyd (lloyd@sun.ac.za).

[W] The online version of this article contains Web-only data.

[OA] Open Access articles can be viewed online without a subscription.

www.plantphysiol.org/cgi/doi/10.1104/pp.110.157776

1998; Farré et al., 2000; Lee et al., 2005). In contrast, tuber-specific plastid-targeted *E. coli* sPPase led to only minor changes in metabolite levels (Farré et al., 2006). In light of the fact that the majority of sPPase activity resides in the plastid (Gross and ap Rees, 1986; Weiner et al., 1987; Gómez-García et al., 2006) and, therefore, relatively low PP<sub>i</sub> levels are maintained (5%–15% of the total cellular PP<sub>i</sub> content is in the plastid compared with approximately 70% in the cytosol; Weiner et al., 1987; Farré et al., 2006), the most likely explanation is that basal plastidial soluble inorganic pyrophosphatase (psPPase) activity tightly governs and efficiently hydrolyzes plastidial PP<sub>i</sub>. In Arabidopsis, a single isoform, *AtPPa6*, with an N-terminal plastid transit peptide extension has been identified (Schulze et al., 2004). Subsequent import (Schulze et al., 2004) and GFP localization studies (Ergen, 2006) have confirmed its subcellular localization. Plastidial PP<sub>i</sub> generation occurs during several metabolic pathways within the chloroplast, for example, chlorophyll, starch, nucleic acid, carotenoid/xanthophyll (Supplemental Fig. S1), and fatty acid and amino acid biosynthesis, and it is hypothesized that these pathways could be severely inhibited if PP<sub>i</sub> is not effectively removed.

Recent studies on key processes in primary metabolism have demonstrated that much still has to be learned about its regulation (Crevillén et al., 2003; Kulma et al., 2004; Kolbe et al., 2005; Sparla et al., 2005; Lunn et al., 2006; Marri et al., 2009; Petreikov et al., 2010), and understanding the influence of PP<sub>i</sub> would expand our knowledge further. Here, we demonstrate that a transient repression of the native *psPPase* gene using virus-induced gene silencing (VIGS) led to increased PP<sub>i</sub> levels associated with altered starch, chlorophyll, carotenoid, malate, and His contents as well as affected photosynthesis in *Nicotiana benthamiana* leaves. Interestingly, events associated with a deficiency in translation of Rubisco were also evident. Furthermore, reduced psPPase led to plants that were less able to cope with drought stress due to an inability to synthesize sufficient abscisic acid (ABA), which leads to an inefficiency to promote stomatal closure. The results presented here suggest that psPPase is essential for the removal of PP<sub>i</sub>, which plays a central role in basic cellular function and maintenance, with little or no metabolic compensation by other plastidial PP<sub>i</sub>-removal mechanisms, demonstrating the importance of this enzyme for maintaining plastidial PP<sub>i</sub> concentrations at low steady-state levels.

## RESULTS

### VIGS Repression of psPPase Activity in *N. benthamiana* Leaves

Sequence analysis of the DNA sequence of At5g09650 (*AtPPa6*) revealed high similarity (75.5%) of the tomato (*Solanum lycopersicum*) EST clone cLET20N17

(GenBank accession no. AW092511.1) to the *AtPPa6* cDNA sequence (Schulze et al., 2004), sharing only between 25.4% and 28.1% identity to the cytosol-targeted *AtPPa1* to *AtPPa5* sequences (Supplemental Fig. S2), thus strongly suggesting that the tomato EST encodes a psPPase. This cDNA was used to produce a vector that is able to induce VIGS of the sPPase encoded by it through ligation of the fragment into the multiple cloning site of the deconstructed TRV2 vector (Liu et al., 2002b). Subsequent coinfiltration with TRV1 and TRV2 (empty or containing the cLET20N17 fragment) into *N. benthamiana* seedlings resulted in reduced total in-gel sPPase activity (Fig. 1A) and an approximate 90% reduction in total sPPase maximal catalytic activity when compared with the TRV2 empty vector controls (Fig. 1C). In order to examine whether the repression was specific to the plastidial isoform, fractions enriched in chloroplast marker enzymes (Supplemental Table S1) were also subjected to an in-gel assay for sPPase activity. A band corresponding to those of the plastidial fraction was significantly reduced in total protein extracts of psPPase-silenced plants (Fig. 1A; Supplemental Fig. S3A). Similarly, immunoblotting using antibodies specifically recognizing the cytosolic isoforms (Rojas-Beltrán et al., 1999) was performed (Fig. 1B) and showed a band of approximately 30 kD that was similar in intensity of extracts from both TRV2 control and psPPase-silenced *N. benthamiana* plants, demonstrating that the VIGS inhibition was specific to psPPase. Lastly, total PP<sub>i</sub> content from leaves of psPPase-silenced and TRV2 control plants was measured and indicated a 3-fold increase in cellular PP<sub>i</sub> in the silenced plants compared with the controls (Fig. 1D).

### Effects of Reduced psPPase Activity on Photosynthesis and Carbon Partitioning between Soluble Sugars and Starch

A striking observation in the TRV2-psPPase plants was the appearance of mottling on the source leaves compared with the control (Fig. 2, A and B). This suggests that pigment accumulation was significantly affected. To further investigate this, chlorophyll, carotenoid, and xanthophyll contents were analyzed by HPLC (Table I). This indicated that the  $\beta$ -carotene, chlorophyll *a* (chl *a*), and violaxanthin contents of psPPase-silenced plants were reduced between 30% and 50% compared with the controls (Table I). In contrast, chlorophyll *b* (chl *b*) and lutein remained invariable from the control, while zeaxanthin content was increased 3-fold in the silenced plants (Table I).

Carbon assimilation was severely impaired in the psPPase-silenced plants (Fig. 2C). At both 380 and 1,000  $\mu\text{mol mol}^{-1}$  CO<sub>2</sub> concentrations, carbon fixation was significantly reduced by 62% and 71%, respectively, in the down-regulated psPPase leaves (Fig. 2C). Starch amounts were also measured and showed a significant decrease in the silenced leaves (Table II). In order to distinguish between a decrease in starch

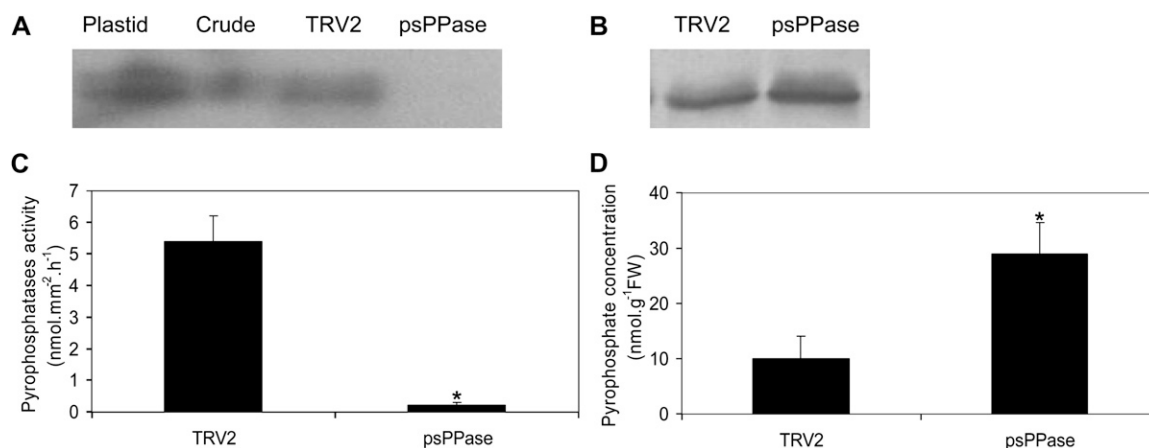


**Figure 1.** Pyrophosphatase activity measurements and  $PP_i$  levels in transiently repressed psPPase in *N. benthamiana* leaves. A, In-gel assays for soluble inorganic pyrophosphatase activity of *N. benthamiana* plastid-enriched fraction (lane 1), crude protein extract (lane 2), infiltrated TRV2 control (lane 3), and TRV2-psPPase-silenced plants (lane 4). B, Immunoblotting of 30  $\mu$ g of crude protein extracts for cytosolic sPPase expression in TRV2 control and psPPase-silenced plants. C, Maximal catalytic pyrophosphatase activity of soluble crude protein extract from TRV2 control and TRV2-psPPase-silenced leaves. D, Total cellular  $PP_i$  concentrations of TRV2 control and TRV2-psPPase-silenced leaves. FW, Fresh weight. Values are presented as means  $\pm$  SE of five individual plants; values with an asterisk were determined by Student's *t* test to be significantly different ( $P < 0.05$ ) from the TRV2 control.

content resulting from increased  $PP_i$  levels and decreased photosynthesis rates, down-regulated psPPase plants were dark adapted for 3 d to allow complete degradation of starch in the leaves. Subsequently, the leaf discs were transferred onto Suc and kept in the dark, and starch content was measured 6 and 24 h after supplementation. Starch levels increased significantly in the TRV2 control plants, while down-regulated psPPase plants could not synthesize starch under these conditions (Fig. 3A). In-gel activity assays for phosphoglucomutase showed no discernible difference between silenced and control plants (Supplemental Fig. S3C), while ADP-Glc pyrophosphorylase activity was increased by approximately 40% in the silenced plants (Fig. 3B). Lastly, soluble sugars levels (Suc, Glc, and Fru) did not change in comparison with the TRV2 control (Table II).

#### Effects of Reduced sPPase Activity on Protein Expression and Metabolite Levels

In light of the fact that a reduction in sPPase led to a significant reduction in plastidial carbon metabolism, it was decided to also investigate protein and metabolite contents following the accumulation of  $PP_i$ . Total soluble protein content expressed on an equal leaf area basis was significantly reduced by approximately 60% in the psPPase plants compared with the controls (Fig. 3C). Furthermore, denaturing protein gels were evaluated for differences in protein-banding patterns between the TRV2 control and psPPase-silenced leaves. Interestingly, the major discernible differences were in the accumulation of both the nucleus- and plastid-encoded Rubisco subunits, which

were greatly reduced in the down-regulated psPPase plants (Fig. 3D). To determine whether the observed effect was due to inhibition of transcription, semi-quantitative reverse transcription (RT)-PCR expression analysis of the two subunits was performed (Fig. 3E). Relative mRNA accumulation values indicated a 30% reduction in the plastid-encoded large subunit of Rubisco (*rbcL*), with no significant change in the nucleus-encoded small subunit of Rubisco (*rbcS*; Fig. 3E).

Nonredundant primary metabolites identified via gas chromatography (GC)-time of flight-mass spectrometry (MS) indicated that glyceraldehyde 3-phosphate, malate, quinate, myo-inositol, Trp, His, Ser, ferulate, coniferylalcohol, 3-caffeoyl quinate, 4-caffeoyl quinate, 5-caffeoyl quinate, and 1-pyrroline-2-carboxylate levels significantly increased in psPPase-silenced plants compared with the respective controls under well-watered conditions. In contrast, citrate levels decreased significantly under the same conditions (Fig. 4; for a full list, see Supplemental Table S2). In light of the fact that an alteration in  $PP_i$  levels could lead to several secondary effects, a linear correlation matrix between prevailing  $PP_i$  levels and the complete subset of primary metabolites was constructed. This indicated highly significant positive correlations between  $PP_i$  levels and ferulate, coniferylalcohol, malate, quinate, His, glyceraldehyde 3-phosphate, and 5-caffeoyl quinate contents ( $r > 0.8$ ), while significant negative correlations between  $PP_i$  levels and chl *a* and  $\beta$ -carotene ( $r > -0.8$ ) contents were observed (Supplemental Table S3).

Due to the precedence of  $PP_i$  utilization as an alternative energy donor, adenylate and uridylylate levels were also determined (Fig. 5). Unfortunately, it was not possible to determine ADP-Glc levels in

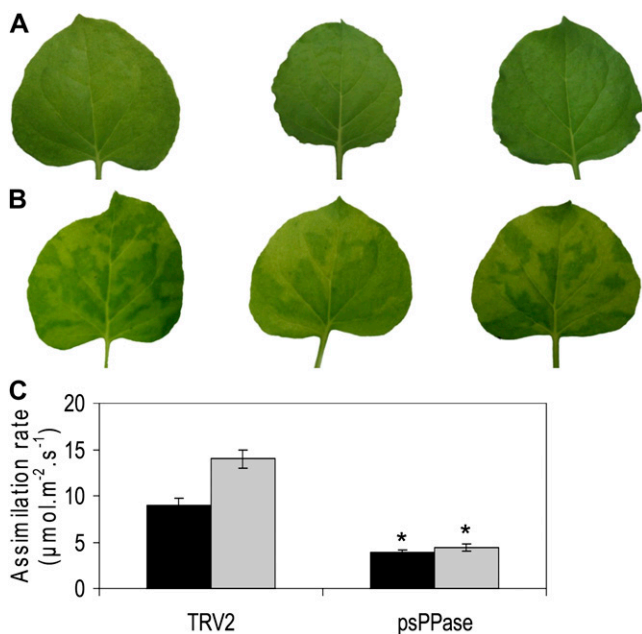


**Figure 2.** Phenotypical characteristics and physiological assessment of carbon assimilation of down-regulated soluble plastidial pyrophosphatase activity in *N. benthamiana* source leaves. A and B, TRV2 control (A) and TRV2-psPPase-silenced (B) leaves grown under prevailing greenhouse conditions. C, Photosynthetic carbon assimilation at both ambient (380  $\mu\text{mol mol}^{-1}$ ; black bars) and saturated (1,000  $\mu\text{mol mol}^{-1}$ ; gray bars) intercellular CO<sub>2</sub> concentrations in TRV2 control and TRV2-psPPase-silenced plants. Values are presented as means  $\pm$  SE of four individual plants; values with an asterisk were determined by Student's *t* test to be significantly different ( $P < 0.05$ ) from the respective TRV2 control.

*N. benthamiana* extracts, making it impossible to establish a direct link between reduced ADP-Glc synthesis and starch accumulation. However, nucleotide levels measured remained either unaltered or were only slightly enhanced for ATP and UDP (Fig. 5, B and C).

#### Effects of PP<sub>i</sub> Metabolism on Drought Tolerance

In order to evaluate the vitality of plants with reduced psPPase activity, a short-term, mild drought stress was induced and phenotypically and biochemically evaluated. Treatment with 10% (w/v) polyethyleneglycol-6000 (water potential ( $\psi_w$ )  $\approx$   $-0.25$  MPa) resulted in an accelerated wilting phenotype in down-regulated psPPase plants compared with the control (Fig. 6A). Stomatal conductance measurements were similar between the control and the down-regulated psPPase plants under well-watered conditions (Fig. 6B); however, the transpiration rate was significantly reduced by approximately 55% in the control and 30% in the psPPase-silenced plants under drought-induced conditions (Fig. 6B). PP<sub>i</sub> concentrations measured under these conditions also indicated a 40% increase in the psPPase plants compared with the TRV2 controls (Fig. 6C). Given this observation, levels of three

key phytohormones, namely ABA, GA<sub>3</sub>, and indole 3-acetic acid (IAA), were measured (Fig. 6, D–F). ABA concentrations increased 3-fold in the drought-stressed control plants, while ABA levels of stressed psPPase plants were unaltered from the well-watered conditions (Fig. 6D). In addition, under drought-induced conditions, both GA<sub>3</sub> and IAA levels increased 2- and 3-fold, respectively, in the psPPase plants (Fig. 6, E and F). Other metabolic constituents, such as soluble sugars (Glc, Fru, and Suc), measured under drought stress were unaffected by the treatment (Table II). On the other hand, starch levels were decreased in psPPase-stressed plants with respect to the stressed control (Table II). Also, the majority of the metabolite changes that were observed for the psPPase-silenced plants under well-watered conditions were also reflected when exposing the TRV2 control to drought stress. psPPase drought-stressed plants revealed few further changes compared with the TRV2-stressed control (Fig. 4; Supplemental Table S2). The exception to this was a significant increase in 2-oxoglutarate levels (Fig. 4).

#### DISCUSSION

Over the past 20 years, PP<sub>i</sub> metabolism has been extensively studied in many species. In microorganisms and invertebrates, it is known that soluble pyrophosphatase activity is necessary for growth and development (Chen et al., 1990; Pérez-Castiñeira et al., 2002; Islam et al., 2005; Ko et al., 2007). Knowledge about the role of PP<sub>i</sub> in plant metabolism, however, remains fragmented. While several attempts have relied on addressing this by removal of PP<sub>i</sub> from a specific subcellular compartment, to our knowledge, no study has been undertaken to examine the effect of PP<sub>i</sub> accumulation in a particular organelle. An Arabidopsis psPPase isoform has been identified (Schulze et al., 2004); however, no insertion mutant in the coding sequence could be identified in various stock centers (RIKEN, SALK,

**Table 1.** Pigment levels of VIGS-infiltrated TRV2 control and psPPase-silenced leaf discs grown under prevailing greenhouse conditions

Values are presented as means  $\pm$  SE of three individual plants, and values in boldface were determined using Student's *t* test to be significantly different ( $P < 0.05$ ) from the TRV2 control. Values are normalized to the internal standard  $\beta$ -apo-caroten-8-al as described in "Materials and Methods."

Pigment	TRV2 Control	psPPase
	<i>response g<sup>-1</sup> fresh wt</i>	
$\beta$ -Carotene	29.7 $\pm$ 0.8	<b>20.9 <math>\pm</math> 2.0</b>
Chl <i>a</i>	504.4 $\pm$ 5.3	<b>377.9 <math>\pm</math> 30.9</b>
Chl <i>b</i>	134.8 $\pm$ 1.8	129.4 $\pm$ 12.9
Lutein	20.4 $\pm$ 0.3	17.4 $\pm$ 2.3
Neoxanthin	2.3 $\pm$ 0.2	2.6 $\pm$ 0.1
Violaxanthin	6.2 $\pm$ 1.0	<b>3.2 <math>\pm</math> 1.1</b>
Zeaxanthin	3.6 $\pm$ 0.0	<b>10.9 <math>\pm</math> 1.5</b>

**Table II.** Effect of down-regulation of psPPase activity on soluble sugar and starch levels of *N. benthamiana* leaves of TRV2 control and TRV2-psPPase-silenced plants under well-watered and drought-induced conditions

Values are presented as means  $\pm$  SE of five individual plants, and values determined to be significantly different ( $P < 0.05$ ) from the respective TRV2 control using Student's *t* test are shown in boldface.

Metabolite	TRV2 Watered	psPPase Watered	TRV2 Drought Stressed	psPPase Drought Stressed
	$\mu\text{mol g}^{-1}$ fresh wt			
Starch	5.5 $\pm$ 1.0	<b>3.0 <math>\pm</math> 0.1</b>	7.5 $\pm$ 1.0	<b>3.0 <math>\pm</math> 1.0</b>
Glc	0.4 $\pm$ 0.1	0.5 $\pm$ 0.1	0.6 $\pm$ 0.2	0.4 $\pm$ 0.1
Fru	0.8 $\pm$ 0.1	1.1 $\pm$ 0.2	1.1 $\pm$ 0.1	0.7 $\pm$ 0.1
Suc	0.9 $\pm$ 0.1	0.8 $\pm$ 0.1	0.9 $\pm$ 0.1	0.8 $\pm$ 0.1

SAIL, GABI-KAT). Because of this, we decided to use VIGS to study the biological role of psPPase in the established *N. benthamiana* posttranscriptional gene-silencing system (Liu et al., 2002b).

Successful silencing of the target protein was confirmed by a 90% decrease in total soluble pyrophosphatase activity, with no discernible effect on cytosolic

sPPase protein expression (Fig. 1, A–C). In addition,  $\text{PP}_i$  levels increased 3-fold (Fig. 1D). Taken together, this demonstrates that a transient repression of the plastidial isoform led to a significant alteration in  $\text{PP}_i$  catabolism in *N. benthamiana* chloroplasts. While  $\text{PP}_i$  accumulation would be expected to significantly perturb pathways generating  $\text{PP}_i$  (Supplemental Fig. S1),

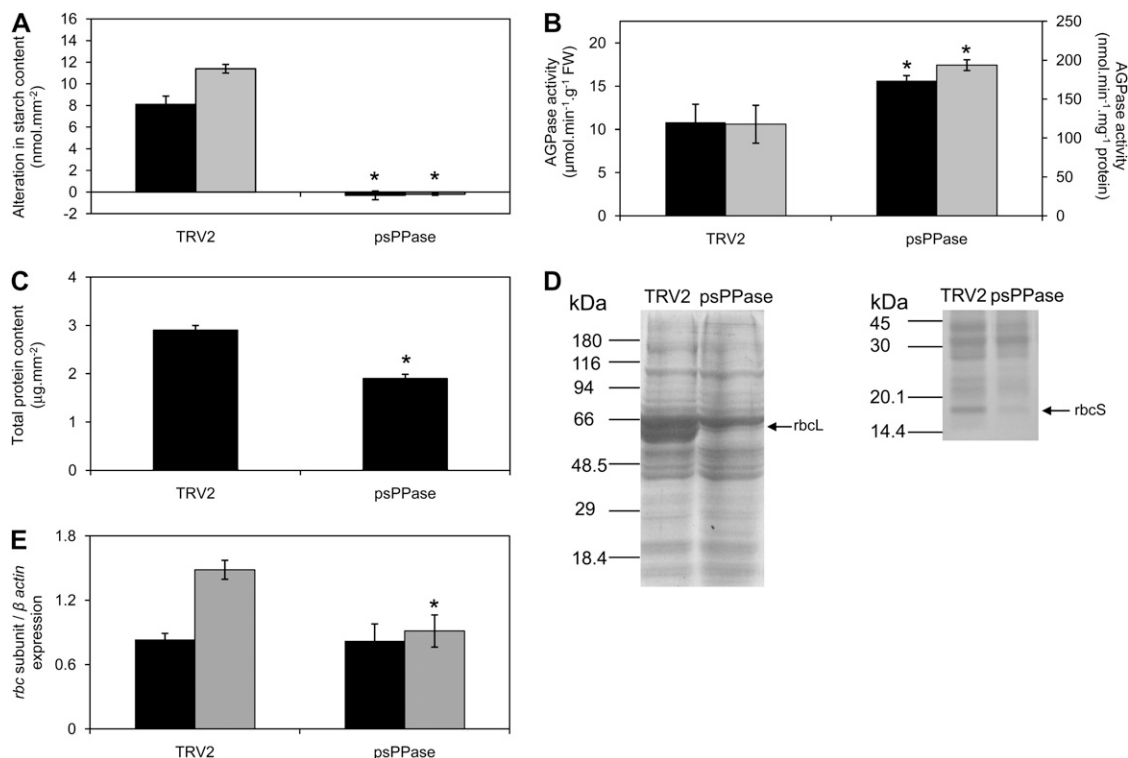
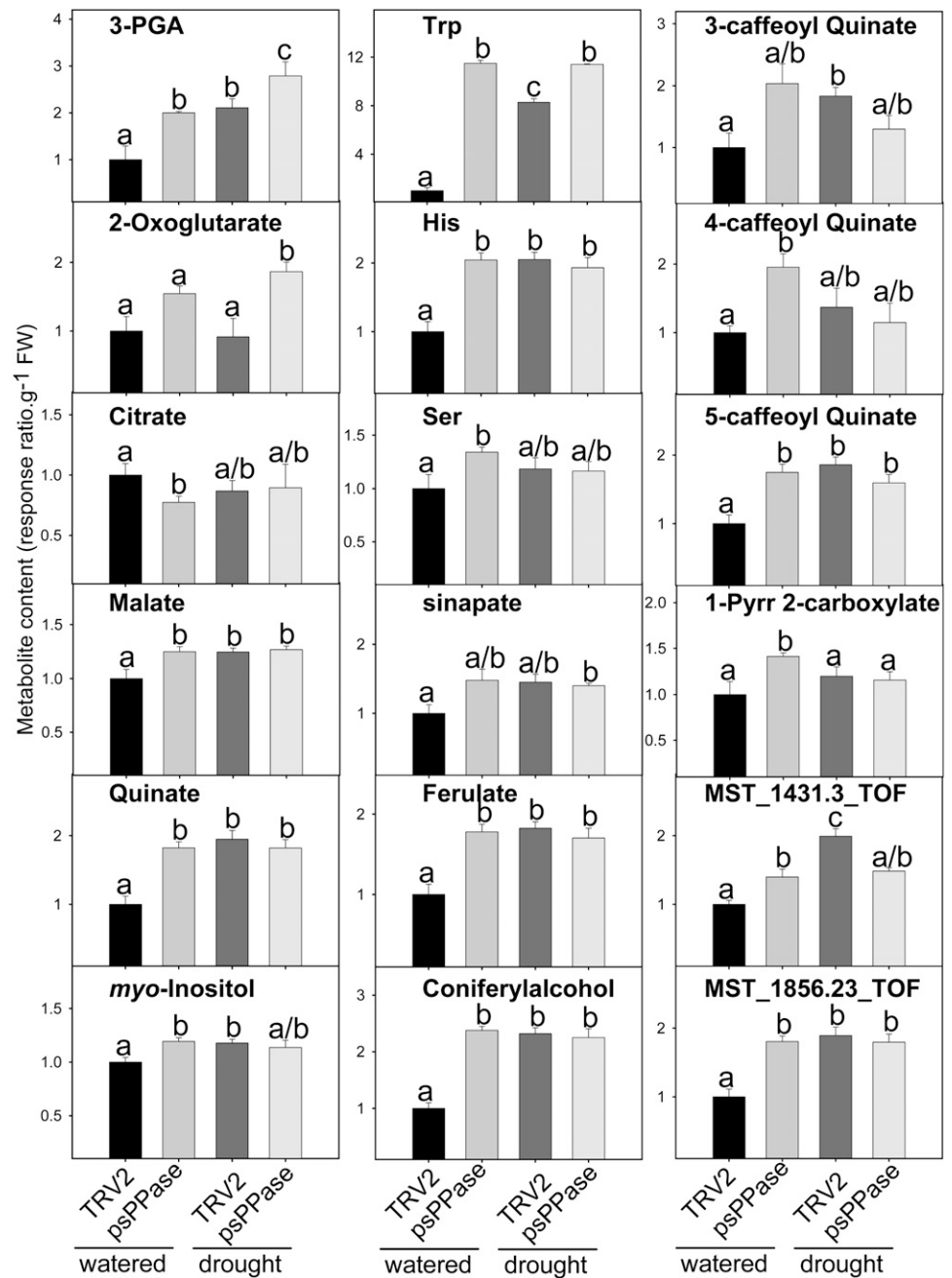


**Figure 3.** Alterations in starch, protein, and Rubisco transcript levels in down-regulated soluble plastidial pyrophosphatase activity in *N. benthamiana* leaves. A, Change in starch content of dark-adapted leaf discs from TRV2 control and silenced plants after 6 h (black bars) and 24 h (gray bar) of incubation on 1.5% (w/v) Suc. B, Maximal catalytic activity of ADP-Glc pyrophosphorylase (AGPase) from TRV2 control and TRV2-psPPase leaf protein extracts expressed in relation to fresh weight (black bars) and total soluble protein (gray bars). FW, Fresh weight. C, Total soluble protein content of leaf discs of TRV2 control and silenced plants. D, Soluble protein amounts of control and psPPase-silenced 64-mm<sup>2</sup> leaf discs, extracted in equal volumes of buffer and 60  $\mu\text{L}$  of supernatant separated on either 10% (w/v; left) or 12% (w/v; right) SDS-PAGE, and stained with Coomassie Brilliant Blue. Molecular mass markers are indicated on the left of each gel. The large (rbcL) and small (rbcS) subunits of Rubisco are indicated by arrows. E, Relative mRNA accumulation of *rbcS* (black bars) and *rbcL* (gray bars) subunits in TRV2 and TRV2-psPPase leaves determined by semiquantitative RT-PCR. Transcript levels are represented as the expression ratio of the respective *rbc* subunit and  $\beta$ -actin gene. Values are presented as means  $\pm$  SE of four/five individual plants; values with an asterisk were determined by Student's *t* test to be significantly different ( $P < 0.05$ ) from the TRV2 control.

**Figure 4.** Relative metabolite content of TRV2 control and TRV2-psPPase plants. Metabolite levels were determined by GC-MS technology. Data are normalized with respect to the mean response calculated for the TRV2 unstressed control (to allow statistical assessment in the same way). Values are presented as means  $\pm$  SE of five individual plants per genotype/treatment, and the data were analyzed using one-way ANOVA followed by Fisher's LSD test; bars that do not share letters are significantly different ( $P < 0.05$ ) from each other. FW, Fresh weight; 3-PGA, 3-phosphoglyceraldehyde; 1-Pyrr 2-carboxylate, 1-pyrroline 2-carboxylate.



and in light of our phenotypical and physiological observations, several essential plastidial components that were affected by this perturbation were identified. These included pigment metabolism, triose phosphate utilization, starch synthesis, and abiotic stress/drought tolerance.

The mottled appearance of light green islands along the leaf adaxial lamina of psPPase-silenced plants (Fig. 2) suggested that isoprenoid biosynthesis could be compromised following PP<sub>i</sub> accumulation. In autotrophic metabolism, isoprenoids act in fundamental roles as photosynthetic pigments (chlorophylls, carotenoids), electron carriers (quinones), radical scavengers (to-

copherols), membrane components (sterols), as well as growth and defense regulators such as ABA, GAs, brassinosteroids, cytokinins, monoterpenes, sesquiterpenes, and diterpenes. Isoprenoids are synthesized from isopentenyl and dimethylallyl diphosphate precursors either in the cytosol via the mevalonate/acetate pathway or through the plastid-localized methylerythritol phosphate pathway (Lichtenthaler, 1999; Supplemental Fig. S1). Plastidial isopentenyl pools have been previously shown to serve primarily as substrate for monoterpenes, diterpenes, tetraterpenes (carotenoids), prenyl moieties of chlorophyll, plastoquinone, and tocopherol as well as having a dual

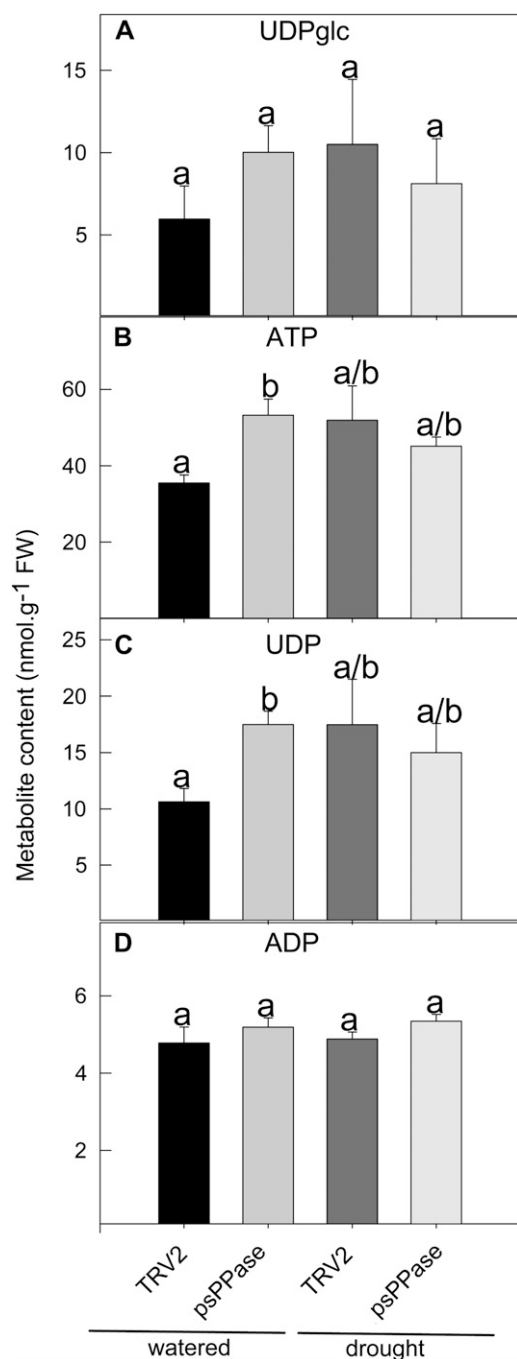


**Figure 5.** Uridinylate and adenylate levels of VIGS-repressed psPPase activity in *N. benthamiana* leaves. UDP-Glc (A), ATP (B), UDP (C), and ADP (D) levels were determined by HPLC. Data are presented as means  $\pm$  SE of four individual plants per treatment. The data were analyzed using one-way ANOVA followed by Fisher's LSD test; bars that do not share letters are significantly different ( $P < 0.05$ ) from each other. FW, Fresh weight.

role with the mevalonate/acetate pathway to supply substrates for sesquiterpene synthesis (Chappell, 2002; Dudareva et al., 2005). The action of the plastid-localized phytoene synthase (Seo and Koshiba, 2002) is reliant on efficient  $PP_i$  dissipation, so its accumulation

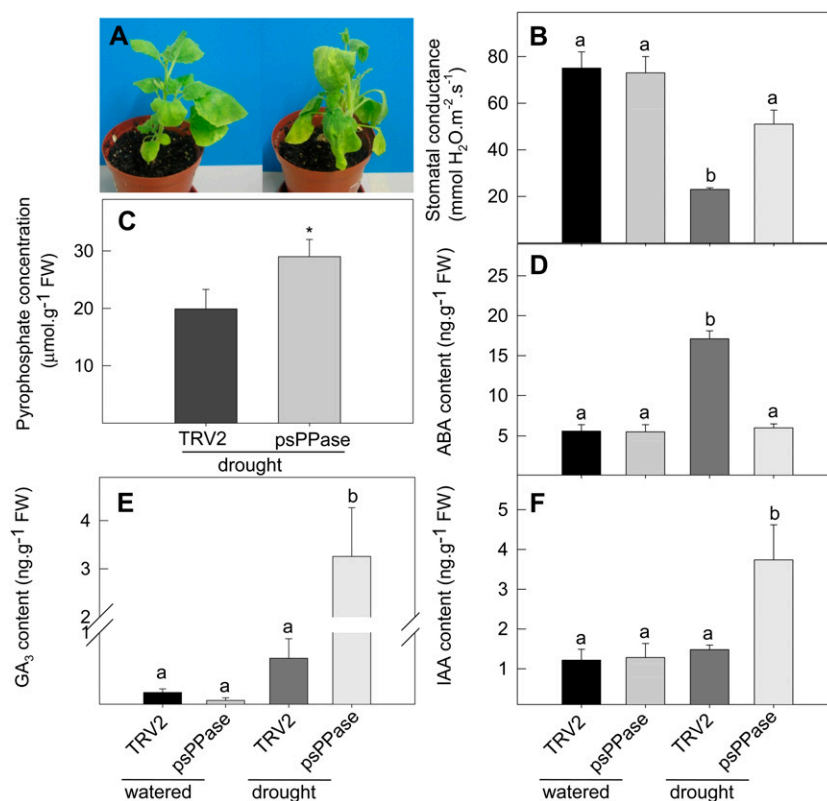
would be expected to affect the synthesis of carotenoids, xanthophylls, ABA, and GAs (Supplemental Fig. S1). In psPPase plants, carotenoid and the phenyl moieties investigated were largely, but not exclusively, down-regulated (Table I).  $\beta$ -Carotene serves as a precursor to the xanthophylls zeaxanthin and violaxanthin. Sunflower (*Helianthus annuus*) deficient in  $\zeta$ -carotene desaturase, an enzyme involved in the early steps of carotenoid biosynthesis, experiences a concurrent decrease in  $\beta$ -carotene, violaxanthin, and chlorophyll contents (Conti et al., 2004), suggesting that substrate availability plays an important role in the levels of these pigments (for review, see Aharoni et al., 2005). In this study, although violaxanthin was decreased, zeaxanthin was increased in the plants with lowered psPPase activity (Table I). Interestingly, both ABA and  $GA_3$  levels remained invariable under unstressed conditions (see below for further discussion), despite the decreases in their precursor molecules.

Chlorophyll is also synthesized in a  $PP_i$ -generating step via chlorophyll synthetase (Supplemental Fig. S1). Chl *a* but not chl *b* amounts were significantly decreased compared with the controls (Table I). This led to a significant decrease in the chl *a/b* ratio (from 3.74 in control to 2.92 in psPPase), suggesting that the stoichiometry of the light-harvesting complex of PSII relative to PSI increased to compensate for the loss in pigment molecules. An alteration in the chl *a/b* ratio has also been suggested to affect retrograde signaling of photosynthetic genes (Pesaresi et al., 2007); however, it is evident from our results that a posttranscriptional mechanism coordinates the accumulation of the Rubisco heteroenzyme subunits (Fig. 3E). A plausible explanation for this is that RNA polymerase and tRNA synthases (both of which produce  $PP_i$ ; Supplemental Fig. S1) are inhibited within the chloroplasts by the  $PP_i$  concentrations in the silenced plants.

The reductions in photosynthetic pigments observed here as well as the reduced amounts of Rubisco suggested that carbon fixation may be affected in the psPPase-silenced plants. Photosynthetic assimilation measurements confirmed that carbon fixation rate was reduced by approximately 55% under ambient  $CO_2$  concentrations (Fig. 3A). The reduction in the photosynthetic rate in the silenced plants could be ruled out as related to phosphate limitation of photosynthesis, due to the fact that the silenced plants do not contain less ATP than controls (Fig. 5B). Reduced photosynthesis under saturating  $CO_2$  concentrations suggests a further limitation in triose phosphate utilization in the psPPase plants. This is supported by an inability of leaf discs to synthesize starch in dark-adapted, Suc-supplemented conditions as well as the enhanced 3-phosphoglycerate levels observed (Figs. 3A and 4). The reduction in carbon fixation is most likely caused by a combination of all of these factors.

As was noted above, the silenced plants in this study were less able to synthesize starch than the controls (Table II; Fig. 3A). A likely explanation for these observations is that the increased  $PP_i$  would affect

**Figure 6.** Physiological and biochemical assessment of drought tolerance in TRV2 control and TRV2-psPPase plants. A, Wilted response of TRV2 control (left) and TRV2-psPPase-silenced (right) plants. B, Stomatal conductance measurements under well-watered and 12-h drought-induced conditions in TRV2 control and TRV2-psPPase-silenced plants. C, PP<sub>i</sub> levels in TRV2 control and TRV2-psPPase-stressed plants. D to F, ABA (D), GA<sub>3</sub> (E), and indole 3-acetic acid (IAA; F) concentrations measured in the leaves under similar conditions under well-watered and stress conditions. Values are presented as means  $\pm$  SE of five individual plants, statistically analyzed using one-way ANOVA followed by Fisher's LSD; bars that do not share letters are significantly different ( $P < 0.05$ ) from each other except for the PP<sub>i</sub> analysis, where a value with an asterisk was determined by Student's *t* test to be significantly different ( $P < 0.05$ ) from the stressed TRV2 control. FW, Fresh weight.



ADP-Glc pyrophosphorylase. This enzyme catalyzes the first committed reaction in starch biosynthesis using Glc-1-P and ATP to produce ADP-Glc and PP<sub>i</sub> (Supplemental Fig. S1) and is known to be essential for starch synthesis. Despite the increase in its activity in crude extracts (Fig. 3B), increased plastidial PP<sub>i</sub> would be expected to make its reaction less thermodynamically favorable in the forward direction *in vivo* (Amir and Cherry, 1972).

When grown under mild drought stress, ABA concentrations were significantly decreased in the psPPase-silenced plants compared with the controls (Fig. 6D). ABA may be synthesized either through a 9-cis-violaxanthin (C40 indirect carotenoid) pathway (mainly found in higher plants; Schwartz et al., 2003) or a farnesyl diphosphate (C15 precursor) pathway (Oritani and Kiyota, 2003). Under drought conditions, ABA is up-regulated and triggers stomatal closure to limit water loss (Mittelheuser and van Steveninck, 1969). In this study, psPPase-repressed plants were characterized by reduced violaxanthin, normal neoxanthin, and increased zeaxanthin contents under prevailing greenhouse conditions (Table I). ABA was also unchanged in the psPPase-repressed plants under normal conditions, and synthesis could not be induced when the plants were challenged with mild water stress. This suggested that stress-induced ABA synthesis in TRV2-psPPase plants is probably derived from violaxanthin. However, it cannot be ruled out that, under water stress conditions, the substrates might become limiting due to compensatory mech-

anisms, whereby pigments are directed toward increasing the photoprotective capacities of the light-harvesting complex (Snyder et al., 2006; Dall'Osto et al., 2007). In accordance with the ABA levels, no difference in transpiration rate between unstressed TRV2-psPPase and TRV2 control plants could be found under normal conditions. The rate decreased in both variants under drought stress; however, the decrease was far less severe in the TRV2-psPPase plants than in the TRV2 controls and led to the TRV2-psPPase plants wilting faster than the respective TRV2 control (Fig. 6, A and B). In addition, it could be speculated that the increased GA<sub>3</sub> and IAA levels in the silenced plants (Fig. 6, E and F) contribute to the reduced ABA biosynthesis through alleviation of DELLA activation of a putative E3 ligase gene (Zentella et al., 2007) or other downstream targets.

In contrast to metabolites that are only evident when exposed to drought-stressed conditions, the TRV2-psPPase plants exhibited a mock drought response under well-watered conditions. These included the increases in metabolite levels of several phenylpropanoids or precursors (quinate, coniferylalcohol, ferulate, 3-caffeoyl quinate, 4-caffeoyl quinate, and 5-caffeoyl quinate), which may be involved in lignification processes associated with drought stress (Lee et al., 2007). Protection against drought stress can also be facilitated by the induction of osmoprotective compounds such as the amino acids Pro and Glu, sugar or sugar polyols, and/or inorganic ions (Mahajan and Tuteja, 2005, and refs. therein). Increases in 1-pyrroline-2-

carboxylate (precursor to Pro), myoinositol, and a metabolite similar to pinitol were also observed in this data set (Fig. 4). When TRV2 control plants were drought induced, the majority of these metabolites accumulated in a similar manner to the TRV2-psPPase unstressed plant and also were not significantly different from the TRV2-psPPase-stressed metabolite levels (Fig. 4). This suggests that  $PP_i$  metabolism might be indirectly involved in mediating drought stress responses in *N. benthamiana* leaves. Interestingly, malate levels also showed similar patterns to those observed for the osmoprotective responses. While the exact mechanism remains unknown, modulation of malate levels in transgenic tomato leaves has been shown to induce opposing photosynthetic responses (Nunes-Nesi et al., 2005, 2007), with anti-sense fumarase plants impaired in regulating stomatal aperture (Nunes-Nesi et al., 2007). Cumulatively, these results suggest that malate plays a profound role in mediating photosynthetic performance and that these responses may also be integrated with the prevailing  $PP_i$  levels.

It remains unclear whether  $PP_i$  is transported across the plastid membrane and whether this could affect metabolism in different compartments. Lunn and Douce (1993) described a transporter from isolated chloroplast preparations that is able to import  $PP_i$  over the chloroplast membrane; however, neither a  $PP_i$  export mechanism nor the corresponding gene has been isolated to date. Similarly, in developing maize (*Zea mays*) embryos, L-malate/ $PP_i$  transport has been demonstrated (Lara-Núñez and Rodríguez-Sotres, 2004), but gene identification remains elusive.

In summary, examining the effect on metabolism of a repression of plastidial pyrophosphatase has demonstrated the essential role that  $PP_i$  plays in many plastidial pathways. Increased  $PP_i$  concentrations led to reduced accumulation of several chloroplast-localized metabolites that are important for plant survival, such as ABA, chlorophyll, and carotenoids. This indicated that repression of psPPase is extremely detrimental to the plant, as photosynthesis is reduced and the plant becomes unable to regulate its water exchanges under mild drought stress due to an inability to manufacture ABA. Taken together, these data indicate that psPPase plays an extremely important role in plastidial metabolism and, similar to microorganisms (Chen et al., 1990; Pérez-Castañeira et al., 2002), we would suggest that a mutation eliminating this soluble pyrophosphatase would be lethal.

## MATERIALS AND METHODS

### VIGS Plasmids for psPPase Transient Repression

The tomato (*Solanum lycopersicum*) EST clone cLET20N17, obtained from the Clemson University Genomics Institute, was digested with *Kpn*I and *Bam*HI and ligated into the same restriction sites in the tobacco mosaic rattle virus vector pTRV2. Deconstructed vectors (pTRV1, pTRV2, and pTRV2-PDS) were transformed into *Agrobacterium tumefaciens* (strain GV2260) by the freeze-thaw method (Höfgen and Willmitzer, 1988).

### Plant Material, Infiltration, and Growth Conditions

*Nicotiana benthamiana* seeds were surface sterilized and germinated on 0.4% (w/v) Plant Gel (Highveld Biotechnology) supplemented with 4.32 g L<sup>-1</sup> Murashige and Skoog basal salt medium (Highveld Biotechnology) and 1.5% (w/v) Suc. Plants were grown in a 16-h/8-h light/dark regime at 24°C. At the four-leaf seedling stage, plants were transferred to 1-L tissue culture containers with the same growth medium constituents for 10 d before being subjected to VIGS infiltration. Seedlings (4–5 weeks after germination) were vacuum infiltrated with 20 mL of transformed *Agrobacterium* suspension (containing a 1:1 mix of TRV1 and either TRV2 or TRV2-psPP). The air volume was adjusted to 20 mL before the nib of the syringe was stoppered. While the leaves of the plant were submerged, the air volume was increased to 40 mL, corresponding to a vacuum of 50 kPa, and held there for 30 s. Infiltrated seedlings were planted and grown in sterile potting soil (with silica and vermiculite [8:1:1]) during the summer months under prevailing greenhouse conditions without any additional carbon supplementation. After 3 weeks, leaves were harvested at midday (unless stated otherwise), immediately frozen in liquid nitrogen, and stored at -80°C until further use. Samples were either whole leaves (leaves 3 to 5) or 64-mm<sup>2</sup> leaf discs taken from leaf 3 using a cork borer and homogenized prior to sample processing. In order to monitor transfection efficiency and growth conditions, the TRV2-PDS vector (containing a cDNA encoding phytoene desaturase; Liu et al., 2002a) was used in parallel as an internal in-house control. All of the phenotypic alterations documented in this paper were observed in at least three independent infiltration experiments.

### Protein Isolation and Determination

Total leaf protein extracts were obtained by vortexing homogenized tissue with ice-cold extraction buffer (50 mM Tris-HCl [pH 7.5], 5 mM dithiothreitol, 2 mM EDTA, and 0.1% [v/v] Triton X-100). Soluble protein extracts were recovered following centrifugation (13,000g for 20 min, 4°C). Protein concentrations were measured according to Bradford (1976) using bovine serum albumin as a standard.

### Plastidial Isolation and Enrichment Determination

Leaf material was harvested from plants that had been destarched by darkening over a 48-h period. Enrichments were then performed according to Kubis et al. (2008). Plastids were collected and centrifuged at 3,000g for 2 min at 4°C, and the pellet was resuspended in 500  $\mu$ L of the protein extraction buffer described above and sonicated for three 1-s bursts separated by 10-s incubations on ice.

### In-Gel sPPase Activity and Denaturing SDS-PAGE Analyses

sPPase in-gel assays were performed by running either total or plastid-enriched protein extracts on a non-denaturing 10% (w/v) polyacrylamide gel at 4°C. The gel was incubated in 20 mL of pyrophosphatase assay buffer as described by Schulze et al. (2004) for 1 h, washed for 5 min in distilled water, before a further 5-min incubation in 1% (w/v) ammonium molybdate, 5% (w/v) FeSO<sub>4</sub>, and 0.5 M H<sub>2</sub>SO<sub>4</sub>. Color development was stopped by washing in excess water.

Soluble proteins were visualized by grinding a 64-mm<sup>2</sup> leaf disc in 200  $\mu$ L of 2% (w/v) SDS, 10% (v/v) glycerol, 5% (v/v)  $\beta$ -mercaptoethanol, 0.002% (w/v) bromophenol blue, and 50 mM Tris-HCl (pH 7.0). Protein extracts were denatured by heating at 95°C for 5 min, and 60  $\mu$ L per sample was separated on a 10% or 12% (w/v) denaturing gel and stained with Coomassie Brilliant Blue.

Immunoblotting of 30  $\mu$ g of protein was performed by denaturing the soluble sample according to Laemmli (1970) prior to separation on a 10% (v/v) SDS-PAGE gel. The proteins were transferred onto a polyvinylidene difluoride membrane (GE Healthcare) using the semidry method (Sambrook et al., 1989) before detection as described previously (Rojas-Beltrán et al., 1999).

### Enzyme Assays

In-gel assays for phosphoglucosyltransferase were performed by loading 30  $\mu$ g of total protein onto a 10% (v/v) native polyacrylamide gel containing 4 mg of glycogen (*Mytilus edulis* type VII; Sigma). The gel was stained according to

Vallejos (1983). Marker enzyme assays were performed to determine the degree of plastid enrichment. For this purpose, nonphosphorylating glyceraldehyde-3-phosphate dehydrogenase (Fernie et al., 2002), ADP-Glc pyrophosphorylase (Sweetlove et al., 1996), UDP-Glc pyrophosphorylase (Sowokinos, 1976), and phosphoenolpyruvate carboxylase (Merlo et al., 1993) activities were determined for plastidial and cytosolic enrichments. Inorganic pyrophosphatase assays were performed as described previously (Schulze et al., 2004).

### Semiquantitative RT-PCR Analysis

Total RNA was isolated from 200 mg of leaf material using the phenol-chloroform method. First-strand cDNA synthesis using oligo(dT) primers was performed on 2  $\mu$ g of DNase-treated RNA using RevertAid H Minus reverse transcriptase according to the manufacturer's instructions (Fermentas). Semiquantitative PCR was performed using BIOTAQ (Bioline) on 0.1  $\mu$ L of cDNA as recommended. The PCR products were separated by electrophoresis on a 1% (w/v) agarose gel, and band intensities were UV light imaged on an Alpha Innotech ChemImager and normalized to the housekeeping gene using AlphaEase FC imaging software (Alpha Innotech). Primer pair combinations that were used are as follows: for *rbc5*, 5'-TTGAAAATGGATGGGTCC-3' / 5'-GCGATGAACTGATGCACTG-3', for *rbcL*, 5'-GCTGCCGAATCTTCTA-CTGG-3' / 5'-ACAGGGGACGACCATACTTG-3'; and for  $\beta$ -actin, 5'-AGATC-CTCACAGACGGTGGT-3' / 5'-CTGCTTCCATTCCGATCATT-3'.

### Drought Stress Treatment

TRV2 control and TRV2-psPPase plants were subjected to a mild drought stress by drenching the root system with 10% (w/v) polyethyleneglycol-6000 for 12 h and subjecting them to phenotypical and biochemical evaluation. Well-watered plants served as a control for each transformant.

### Stomatal Conductance and Carbon Assimilation Rates

Stomatal conductance was measured on an EGM-4 Environmental Gas Monitor (PP Systems). Readings were taken directly prior to harvesting at midday on the fourth leaf of each plant with the flow rate (50 mL min<sup>-1</sup>) and temperature (25°C) kept constant. Carbon assimilation rates were analyzed using an infrared gas analyzer (Ciras-1; PP Systems) on the third fully expanded leaf from psPPase and control plants at 0, 380, and 1,000  $\mu$ mol mol<sup>-1</sup> intercellular CO<sub>2</sub> concentrations with a flow rate of 350 mL min<sup>-1</sup>, 25°C, and constant photosynthetically active radiation of 1,400  $\mu$ mol m<sup>-2</sup> s<sup>-1</sup>.

### Metabolite Determinations

PP<sub>i</sub> was extracted from leaf tissue by the TCA/ether method (Jelitto et al., 1992). PP<sub>i</sub> was determined using the colorimetric PiPer PP<sub>i</sub> cycling assay kit (Invitrogen) according to the manufacturer's specifications. All porcelain and glassware were pretreated overnight with 0.1 M HCl to remove residual phosphate. PP<sub>i</sub> levels were determined by a sample blank with or without sPPase, and total P<sub>i</sub> was calculated by comparison of fluorescence at 595 nm with a linear P<sub>i</sub> standard curve.

Soluble sugars and starch were extracted and assayed according to Müller-Röber et al. (1992).

Primary metabolite levels were extracted and derivatized as described previously (Roessner et al., 2001), and GC-MS evaluation was according to Erban et al. (2007). Data integration and quantification were processed using TagFinder software (Luedemann et al., 2008) by integrating libraries housed in the Golm metabolome database (Kopka et al., 2005; Schauer et al., 2005).

Adenylates and uridinylates were extracted and detected as described by Fernie et al. (2001).

Carotenoids and xanthophylls was extracted and determined according to Taylor et al. (2006). Homogenized leaf discs were incubated for 5 min with 100  $\mu$ L of methanol containing  $\beta$ -apo-caroten-8-al as an internal standard, 100  $\mu$ L of 50 mM Tris-HCl (pH 8.0), and 1 M NaCl added and incubated for another 5 min. The mixture was partitioned twice with 400  $\mu$ L of chloroform and centrifuged at 3,000g for 5 min at 4°C, and the lower phases were pooled and dried under vacuum. Samples were immediately resuspended in ethyl acetate:methanol (1:4) with 0.1% (w/v) butylated hydroxytoluene and run according to Taylor et al. (2006). The peak area was integrated and normalized with respect to 53.5 ng of  $\beta$ -apo-caroten-8-al injected.

### Phytohormone Profiling

Phytohormones were extracted according to Edlund et al. (1995). In brief, 500  $\mu$ L of 0.05 M Na-phosphate buffer (pH 7.0) was added in a 10:1 ratio to homogenized leaf tissue and incubated for 1 h in the dark with continuous shaking at 4°C. After extraction, the pH was adjusted to 2.6, and the sample was enriched with approximately 35 mg of Amberlite XAD-7 (Serva) and further incubated for 1 h in the dark with continuous shaking at 4°C. After centrifugation, the XAD-7 was washed twice with 500  $\mu$ L of 1% (v/v) acetic acid before elution with 500  $\mu$ L of dichloromethane for 30 min, and elution was repeated once more. The combined dichloromethane fractions were reduced under vacuum until dry. Derivatization of the sample (modified from Schmelz et al., 2003) was achieved by adding 50  $\mu$ L of 2.0 M trimethylsilyl diazomethane in hexane (Sigma-Aldrich) and 10  $\mu$ L of methanol and incubating at room temperature for 30 min. Excess trimethylsilyl diazomethane was destroyed by adding 50  $\mu$ L of 1% acetic acid. *n*-Alkane time standards were added to each sample prior to reducing the sample to dryness under vacuum. Samples were resuspended in 50  $\mu$ L of heptane and injected splitless into a GCT Premier benchtop orthogonal acceleration time-of-flight MS apparatus (Waters). Running conditions were exactly as described previously (Edlund et al., 1995), phytohormone identification and quantification were done by means of linear calibration curves for authentic standards, and the mass spectra were adjusted accordingly.

### Statistical Analysis

Unless otherwise specified, statistical analyses were performed using Student's *t* test embedded in the Microsoft Excel software. Only the return of a value of *P* < 0.05 was designated significant. ANOVA followed by Fisher's LSD test was conducted either in Statistica 8 (StatSoft), SPSS, or R 2.10.0 software (R Development Core Team, 2009), and the return of a value of *P* < 0.05 was designated significant. Linear correlations were performed with the partial least-square regression algorithm embedded in the XLSTAT software for Microsoft Excel at a 95% confidence level. cDNA sequence analysis was performed using the ClustalW2 algorithm (Larkin et al., 2007).

Sequence data from this article can be found in the GenBank/EMBL data libraries under accession numbers NM\_099987.3, NM\_127380.3, NM\_130253.2, NM\_115222.2, NM\_116378.3, and NM\_121002.3 for *AtPPa1* to *AtPPa6*, respectively, as well as AW092511 for cLET20N17.

### Supplemental Data

The following materials are available in the online version of this article.

**Supplemental Figure S1.** Schematic representation of selected plastidial reactions generating PP<sub>i</sub>.

**Supplemental Figure S2.** Dendrogram of the Arabidopsis cytosolic and plastidial sPPases and the tomato EST clone, cLET20N17.

**Supplemental Figure S3.** Protein expression in TRV2 control and TRV2-psPPase plants.

**Supplemental Table S1.** Marker enzyme activities following chloroplast isolation.

**Supplemental Table S2.** Full list of relative metabolite contents of TRV2 control and TRV2-psPPase-silenced plants.

**Supplemental Table S3.** Linear correlation matrix of PP<sub>i</sub>, primary metabolite, and ABA levels.

### ACKNOWLEDGMENTS

We are grateful for kind gifts of TRV1, TRV2, and TRV2-PDS vectors from Savithramma Dinesh-Kumar (Yale University), cytosolic soluble pyrophosphatase antibody from Uwe Sonnewald (Friedrich Alexander University; originally produced by Patrick du Jardin [Gembloux Agricultural University]), and a GA mass spectrum library from Peter Hedden (Rothamstead Research). HPLC analysis of pigments was performed by Justin Lashbrooke (University of Stellenbosch). Bénédicte Lebouteiller helped with the design of RT-PCR primers, while technical assistance was kindly offered by Ebrahim Samodien and Christelle Cronje (all from University of Stellenbosch).

Received April 14, 2010; accepted July 2, 2010; published July 6, 2010.

## LITERATURE CITED

- Aharoni A, Jongsma MA, Bouwmeester HJ (2005) Volatile science? Metabolic engineering of terpenoids in plants. *Trends Plant Sci* **10**: 594–602
- Amir J, Cherry JH (1972) Purification and properties of adenosine diphosphoglucose pyrophosphorylase from sweet corn. *Plant Physiol* **49**: 893–897
- Baltscheffsky M, Schultz A, Baltscheffsky H (1999) H<sup>+</sup>-PPases: a tightly membrane-bound family. *FEBS Lett* **457**: 527–533
- Bradford MM (1976) A rapid and sensitive method for quantitation of microgram quantities of protein utilizing the principle of protein-dye-binding. *Anal Biochem* **72**: 248–252
- Chappell J (2002) The genetics and molecular genetics of terpene and sterol origami. *Curr Opin Plant Biol* **5**: 151–157
- Chen J, Brevet A, Fromant M, Lévêque F, Schmitter JM, Blanquet S, Plateau P (1990) Pyrophosphatase is essential for growth of *Escherichia coli*. *J Bacteriol* **172**: 5686–5689
- Conti A, Pancaldi S, Fambrini M, Michelotti V, Bonora A, Salvini M, Pugliesi C (2004) A deficiency at the gene coding for  $\zeta$ -carotene desaturase characterizes the sunflower *non dormant-1* mutant. *Plant Cell Physiol* **45**: 445–455
- Crebillén P, Ballicora MA, Mérida A, Preiss J, Romero JM (2003) The different large subunit isoforms of *Arabidopsis thaliana* ADP-glucose pyrophosphorylase confer distinct kinetic and regulatory properties to the heterotetrameric enzyme. *J Biol Chem* **278**: 28508–28515
- Dall’Osto L, Cazzaniga S, North H, Marion-Poll A, Bassi R (2007) The *Arabidopsis aba4-1* mutant reveals a specific function for neoxanthin in protection against photooxidative stress. *Plant Cell* **19**: 1048–1064
- Dudareva N, Andersson S, Orlova I, Gatto N, Reichelt M, Rhodes D, Boland W, Gershenzon J (2005) The nonmevalonate pathway supports both monoterpene and sesquiterpene formation in snapdragon flowers. *Proc Natl Acad Sci USA* **102**: 933–938
- Edlund A, Eklof S, Sundberg B, Moritz T, Sandberg G (1995) A microscale technique for gas chromatography-mass spectrometry measurements of picogram amounts of indole-3-acetic acid in plant tissues. *Plant Physiol* **108**: 1043–1047
- Erbán A, Schauer N, Fernie AR, Kopka J (2007) Non-supervised construction and application of mass spectral and retention time index libraries from time-of-flight GC-MS metabolite profiles. In W Weckwerth, ed, *Metabolomics: Methods and Protocols*. Humana Press, Totowa, NJ, pp 19–38
- Ergen ZN (2006) A functional genomics approach to the plant soluble pyrophosphatase family. PhD thesis. Ruprecht-Karl University, Heidelberg
- Farré EM, Geigenberger P, Willmitzer L, Trethewey RN (2000) A possible role for pyrophosphate in the coordination of cytosolic and plastidial carbon metabolism within the potato tuber. *Plant Physiol* **123**: 681–688
- Farré EM, Tech S, Trethewey RN, Fernie AR, Willmitzer L (2006) Subcellular pyrophosphate metabolism in developing tubers of potato (*Solanum tuberosum*). *Plant Mol Biol* **62**: 165–179
- Farré EM, Tiessen A, Roessner U, Geigenberger P, Trethewey RN, Willmitzer L (2001) Analysis of the compartmentation of glycolytic intermediates, nucleotides, sugars, organic acids, amino acids, and sugar alcohols in potato tubers using a nonaqueous fractionation method. *Plant Physiol* **127**: 685–700
- Fernie AR, Roessner U, Trethewey RN, Willmitzer L (2001) The contribution of plastidial phosphoglucomutase to the control of starch synthesis within the potato tuber. *Planta* **213**: 418–426
- Fernie AR, Roscher A, Ratcliffe RG, Kruger NJ (2002) Activation of pyrophosphate:fructose-6-phosphate 1-phosphotransferase by fructose 2,6-bisphosphatase stimulates conversion of hexose phosphates to triose phosphates but does not influence accumulation of carbohydrates in phosphate-deficient tobacco cells. *Physiol Plant* **114**: 172–181
- Geigenberger P, Hajirezaei M, Geiger M, Deiting U, Sonnewald U, Stitt M (1998) Overexpression of pyrophosphatase leads to increased sucrose degradation and starch synthesis, increased activities of enzymes for sucrose-starch interconversions, and increased levels of nucleotides in growing potato tubers. *Planta* **205**: 428–437
- Gómez-García MR, Losada M, Serrano A (2006) A novel subfamily of monomeric inorganic pyrophosphatases in photosynthetic eukaryotes. *Biochem J* **395**: 211–221
- Gross P, ap Rees T (1986) Alkaline inorganic pyrophosphatase and starch synthesis in amyloplasts. *Planta* **167**: 140–145
- Hajirezaei M, Sonnewald U, Viola R, Carlisle S, Dennis DT, Stitt M (1994) Transgenic potato plants with strongly decreased expression of pyrophosphate:fructose-6-phosphate phosphotransferase show no visible phenotype and only minor changes in metabolic fluxes in their tubers. *Planta* **192**: 16–30
- Höfgen R, Willmitzer L (1988) Storage of competent cells for *Agrobacterium* transformation. *Nucleic Acids Res* **16**: 9877
- Islam MK, Miyoshi T, Yamada M, Tsuji N (2005) Pyrophosphatase of the roundworm *Ascaris suum* plays an essential role in the worm’s molting and development. *Infect Immun* **73**: 1995–2004
- Jelitto T, Sonnewald U, Willmitzer L, Hajirezaei M, Stitt M (1992) Inorganic pyrophosphate content and metabolites in potato and tobacco plants expressing *E. coli* pyrophosphatase in their cytosol. *Planta* **188**: 238–244
- Jiang SS, Fan LL, Yang SJ, Kuo SY, Pan RL (1997) Purification and characterization of thylakoid membrane-bound inorganic pyrophosphatase from *Spinacia oleracea* L. *Arch Biochem Biophys* **346**: 105–112
- Ko KM, Lee W, Yu JR, Ahnn J (2007) PYP-1, inorganic pyrophosphatase, is required for larval development and intestinal function in *C. elegans*. *FEBS Lett* **581**: 5445–5453
- Kolbe A, Tiessen A, Schlupepmann H, Paul M, Ulrich S, Geigenberger P (2005) Trehalose 6-phosphate regulates starch synthesis via posttranslational redox activation of ADP-glucose pyrophosphorylase. *Proc Natl Acad Sci USA* **102**: 11118–11123
- Kopka J, Schauer N, Krueger S, Birkemeyer C, Usadel B, Bergmüller E, Dormann P, Weckwerth W, Gibon Y, Stitt M, et al (2005) GMD@CSB. DB: the Golm metabolome database. *Bioinformatics* **21**: 1635–1638
- Kubis SE, Lilley KS, Jarvis P (2008) Isolation and preparation of chloroplasts from *Arabidopsis thaliana* plants. *Methods Mol Biol* **425**: 171–186
- Kulma A, Villadsen D, Campbell DG, Meek SEM, Harthill JE, Nielsen TM, MacKintosh C (2004) Phosphorylation and 14-3-3 binding of Arabidopsis 6-phosphofructo-2-kinase/fructose-2,6-bisphosphatase. *Plant J* **37**: 654–667
- Laemmli UK (1970) Cleavage of structural proteins during the assembly of the head of bacteriophage T4. *Nature* **227**: 680–685
- Lara-Núñez A, Rodríguez-Sotres R (2004) Characterization of a dicarboxylate exchange system able to exchange pyrophosphate for L-malate in non-photosynthetic plastids from developing maize embryos. *Plant Sci* **166**: 1335–1343
- Larkin MA, Blackshields G, Brown NP, Chenna R, McGettigan PA, McWilliam H, Valentin F, Wallace IM, Wilm A, Lopez R, et al (2007) ClustalW and ClustalX version 2. *Bioinformatics* **23**: 2947–2948
- Lee BR, Kim KY, Jung WJ, Avice JC, Ourry A, Kim TH (2007) Peroxidases and lignification in relation to the intensity of water-deficit stress in white clover (*Trifolium repens* L.). *J Exp Bot* **58**: 1271–1279
- Lee JW, Lee DS, Bhoo SH, Jeon JS, Lee YH, Hahn TR (2005) Transgenic Arabidopsis plants expressing *Escherichia coli* pyrophosphatase display both altered carbon partitioning in their source leaves and reduced photosynthetic activity. *Plant Cell Rep* **24**: 374–382
- Lichtenthaler HK (1999) The 1-deoxy-D-xylulose-5-phosphate pathway of isoprenoid biosynthesis in plants. *Annu Rev Plant Physiol Plant Mol Biol* **50**: 47–65
- Liu Y, Schiff M, Dinesh-Kumar SP (2002a) Virus-induced gene silencing in tomato. *Plant J* **31**: 777–786
- Liu Y, Schiff M, Marathe R, Dinesh-Kumar SP (2002b) Tobacco *Rar1*, *EDS1* and *NPR1/NIM1* like genes are required for N-mediated resistance to tobacco mosaic virus. *Plant J* **30**: 415–429
- López-Marqués RL, Pérez-Castiñeira JR, Losada M, Serrano A (2004) Differential regulation of soluble and membrane-bound inorganic pyrophosphatases in the photosynthetic bacterium *Rhodospirillum rubrum* provides insights into pyrophosphate-based stress bioenergetics. *J Bacteriol* **186**: 5418–5426
- Luedemann A, Strassburg K, Alexander E, Kopka J (2008) TagFinder for the quantitative analysis of gas chromatography-mass spectrometry (GC-MS) based metabolite profiling experiments. *Bioinformatics* **24**: 732–737
- Lunn JE, Douce R (1993) Transport of inorganic pyrophosphate across the spinach chloroplast envelope. *Biochem J* **290**: 375–379
- Lunn JE, Feil R, Hendriks JH, Gibon Y, Morcuende R, Osuna D, Scheible WR, Carillo P, Hajirezaei MR, Stitt M (2006) Sugar-induced increases in trehalose 6-phosphate are correlated with redox activation of ADP-glucose pyrophosphorylase and higher rates of starch synthesis in *Arabidopsis thaliana*. *Biochem J* **397**: 139–148

- Maeshima M** (2000) Vacuolar H(+)-pyrophosphatase. *Biochim Biophys Acta* **1465**: 37–51
- Mahajan S, Tuteja N** (2005) Cold, salinity and drought stresses: an overview. *Arch Biochem Biophys* **444**: 139–158
- Marri L, Zaffagnini M, Collin V, Issakidis-Bourguet E, Lemaire SD, Pupillo P, Sparla F, Miginiac-Maslow M, Trost P** (2009) Prompt and easy activation by specific thioredoxins of Calvin cycle enzymes of *Arabidopsis thaliana* associated in the GAPDH/CP12/PRK supramolecular complex. *Mol Plant* **2**: 259–269
- Merlo L, Geigenberger P, Hajirezaei M, Stitt M** (1993) Changes in carbohydrates, metabolites and enzyme activities in potato tubers during development and within a single tuber along the stolon-apex gradient. *J Plant Physiol* **142**: 392–402
- Mittelheuser CJ, van Steveninck RFM** (1969) Stomatal closure and inhibition of transpiration induced by (RS)-abscisic acid. *Nature* **221**: 281–282
- Müller-Röber B, Sonnwald U, Willmitzer L** (1992) Inhibition of the ADP-glucose pyrophosphorylase in transgenic potatoes leads to sugar-storing tubers and influences tuber formation and expression of tuber storage protein genes. *EMBO J* **11**: 1229–1238
- Nunes-Nesi A, Carrari F, Gibon Y, Sulpice R, Lytovchenko A, Fisahn J, Graham J, Ratcliffe RG, Sweetlove LJ, Fernie AR** (2007) Deficiency of mitochondrial fumarate activity in tomato plants impairs photosynthesis via an effect on stomatal function. *Plant J* **50**: 1093–1106
- Nunes-Nesi A, Carrari F, Lytovchenko A, Smith AM, Loureiro ME, Ratcliffe RG, Sweetlove LJ, Fernie AR** (2005) Enhanced photosynthetic performance and growth as a consequence of decreasing mitochondrial malate dehydrogenase activity in transgenic tomato plants. *Plant Physiol* **137**: 611–622
- Oritani T, Kiyota H** (2003) Biosynthesis and metabolism of abscisic acid and related compounds. *Nat Prod Rep* **20**: 414–425
- Paul M, Sonnwald U, Hajirezaei M, Dennis D, Stitt M** (1995) Transgenic tobacco plants with strongly decreased expression of pyrophosphate: fructose-6-phosphate 1-phosphotransferase do not differ significantly from wild type in photosynthate partitioning, plant growth or their ability to cope with limiting phosphate, limiting nitrogen and suboptimal temperatures. *Planta* **196**: 277–283
- Pérez-Castiñeira JR, López-Marqués RL, Villalba JM, Losada M, Serrano A** (2002) Functional complementation of yeast cytosolic pyrophosphatase by bacterial and plant H<sup>+</sup>-translocating pyrophosphatases. *Proc Natl Acad Sci USA* **99**: 15914–15919
- Pesaresi P, Schneider A, Kleine T, Leister D** (2007) Interorganellar communication. *Curr Opin Plant Biol* **10**: 600–606
- Petrekov M, Eisenstein M, Yeselason Y, Preiss J, Schaffer AA** (2010) Characterization of the AGPase large subunit isoforms from tomato indicates that the recombinant L3 subunit is active as a monomer. *Biochem J* **428**: 201–212
- R Development Core Team** (2009) R: A Language and Environment for Statistical Computing. R Foundation for Statistical Computing, Vienna
- Rea PA, Poole RJ** (1993) Vacuolar H<sup>+</sup>-translocating pyrophosphatase. *Annu Rev Plant Physiol Plant Mol Biol* **44**: 157–180
- Roessner U, Willmitzer L, Fernie AR** (2001) High-resolution metabolic phenotyping of genetically and environmentally diverse potato tuber systems: identification of phenocopies. *Plant Physiol* **127**: 749–764
- Rojas-Beltrán JA, Dubois E, Mortiaux E, Portetelle D, Gebhardt C, Sangwan RS, du Jardin P** (1999) Identification of cytosolic Mg<sup>2+</sup>-dependent soluble inorganic pyrophosphatases in potato and phylogenetic analysis. *Plant Mol Biol* **39**: 449–461
- Sambrook J, Fritsch EF, Maniatis T** (1989) *Molecular Cloning: A Laboratory Manual*, Ed 2. Cold Spring Harbor Laboratory Press, Cold Spring Harbor, NY, pp 18.47–18.61
- Schauer N, Steinhäuser D, Strelkov S, Schomburg D, Allison G, Moritz T, Lundgren K, Roessner-Tunali U, Forbes MG, Willmitzer L, et al** (2005) GC-MS libraries for the rapid identification of metabolites in complex biological samples. *FEBS Lett* **579**: 1332–1337
- Schmelz EA, Engelberth J, Alborn HT, O'Donnell P, Sammons M, Toshima H, Tumlinson JH III** (2003) Simultaneous analysis of phytohormones, phytotoxins, and volatile organic compounds in plants. *Proc Natl Acad Sci USA* **100**: 10552–10557
- Schulze S, Mant A, Kossmann J, Lloyd J** (2004) Identification of an *Arabidopsis* inorganic pyrophosphatase capable of being imported into the chloroplast. *FEBS Lett* **565**: 101–105
- Schwartz SH, Qin X, Zeevaart JAD** (2003) Elucidation of the indirect pathway of abscisic acid biosynthesis by mutants, genes and enzymes. *Plant Physiol* **131**: 1591–1601
- Seo M, Koshiba T** (2002) Complex regulation of ABA biosynthesis in plants. *Trends Plant Sci* **7**: 41–48
- Snyder AM, Clark BM, Robert B, Ruban AV, Bungard RA** (2006) Carotenoid specificity of light-harvesting complex II binding sites: occurrence of 9-cis-violaxanthin in the neoxanthin-binding site in the parasitic angiosperm *Cuscuta reflexa*. *J Biol Chem* **279**: 5162–5168
- Sonnwald U** (1992) Expression of *E. coli* inorganic pyrophosphatase in transgenic plants alters photoassimilate partitioning. *Plant J* **2**: 571–581
- Sonnwald U** (2001) Control of potato tuber sprouting. *Trends Plant Sci* **6**: 333–335
- Sowokinos JR** (1976) Phosphorylases in *Solanum tuberosum*. I. Changes in ADP-glucose pyrophosphorylase and UDP-glucose pyrophosphorylase activities associated with starch biosynthesis during tuberization, maturation, and storage of potatoes. *Plant Physiol* **57**: 63–68
- Sparla F, Zaffagnini M, Wedel N, Scheibe R, Pupillo P, Trost P** (2005) Regulation of photosynthetic GAPDH dissected by mutants. *Plant Physiol* **138**: 2210–2219
- Stitt M** (1998) Pyrophosphate as an energy donor in the cytosol of plant cells: an enigmatic alternative to ATP. *Bot Acta* **111**: 167–175
- Sweetlove LJ, Burrell MM, ap Rees T** (1996) Characterization of transgenic potato (*Solanum tuberosum*) tubers with increased ADPglucose pyrophosphorylase. *Biochem J* **320**: 487–492
- Taylor KL, Brackenridge AE, Vivier MA, Oberholster A** (2006) High-performance liquid chromatography profiling of the major carotenoids in *Arabidopsis thaliana* leaf tissue. *J Chromatogr A* **1121**: 83–91
- Vallejos CE** (1983) Enzyme activity staining. In SD Tanksley, TJ Orton, eds, *Isozymes in Plant Genetics and Breeding: Part A*. Elsevier, Amsterdam, pp 469–516
- Vianello A, Macrì F** (1999) Proton pumping pyrophosphatase from higher plant mitochondria. *Physiol Plant* **105**: 763–768
- Weiner H, Stitt M, Heldt HW** (1987) Subcellular compartmentation of pyrophosphate and alkaline pyrophosphatase in leaves. *Biochim Biophys Acta* **893**: 13–21
- Zentella R, Zhang ZL, Park M, Thomas SG, Endo A, Murase K, Fleet CM, Jikumaru Y, Nambara E, Kamiya Y, et al** (2007) Global analysis of DELLA direct targets in early gibberellin signaling in *Arabidopsis*. *Plant Cell* **19**: 3037–3057